J. Indian Inst. Sci., Jan.–Feb. 1987, **67**, pp. 51–63.

IISc THESES ABSTRACTS

Thesis Abstract (Ph.D.)

Electron spectroscopic studies of surface segregation and oxidation of Cu- and Ni-based alloys and low temperature preparation and characterisation of intermetallics based on the system Fe-W-Mo by T. S. Sampath Kumar.
Research supervisors: M. S. Hegde and R. M. Mallya.
Department: Metallurgy (Under Materials Science interdisciplinary research programme).

1. Introduction

Reactivity of alloy surfaces with special reference to catalysis and corrosion is of current interest in surface science. Often the surface composition of an alloy is different from that of the bulk and this phenomenon is known as surface segregation[1]. Modern surface analytical techniques such as X-ray photoelectron spectroscopy (XPS), UV photoelectron spectroscopy (UPS) and Auger electron spectroscopy (AES) can be fruitfully employed to study surface segregation and oxidation, a typical surface reaction[2]. In the present study, under the materials science research programme, surface segregation and oxidation of Cu- and Ni-based, mostly polycrystalline, single-phase binary alloys have been studied employing electron spectroscopy (XPS, UPS and AES) and thermal desorption spectroscopy (TDS). The intermetallics, Fe_2W, FeMo and others of the Fe-W-Mo system have also been prepared by hydrogen reduction of the respective oxides (prepared by ceramic method) at a relatively low temperature for the first time. These intermetallics and their oxide precursors have been similarly characterised.

2. Preparation and characterisation

Solid-solution alloys such as Cu-5at.%Mn were melted in an induction or arc furnace under vacuum or inert atmosphere as required. The structure and phase of the alloys were confirmed by X-ray powder diffraction and by metallography, while the composition was determined by electron probe microanalysis and chemical analysis. Mössbauer spectroscopy and XPS were used to characterise the electronic structure of the oxides and intermetallics, and Mössbauer studies were conducted in some cases for the first time.

3. Surface segregation

Identification of the segregating component and its concentration variation with temperature (300 to 800 K) have been carried out in segregation studies, by following the metal core level intensities from XPS as well as from Auger spectroscopy. Surface segregation of Mn, Ge, Sn and In has been observed in Cu-5at.%Mn, Cu-5at.%Ge, Cu-1at.%Sn and Cu-1at.%In alloys, whereas Cu segregation is seen in the case of Cu-9at.%Pd and Cu-25at.%Pd alloys (fig. 1). All the

nickel-based alloys studied, *viz.*, Ni-5at.%Mn, Ni-5at.%Ge and Ni-4.96at.%Ru showed surface segregation of their solutes, *i.e.*, Mn, Ge and Ru respectively. Segregation of Sn and Ni has been observed in the ternary Cu-9.7at.%Ni-2.3at.%Sn alloy in addition to evidence of site competition between Ni and Sn, unlike that in the Cu-Sn binary alloy. Apparent enthalpies of segregation have been obtained from the Arrhenius plots of the surface composition ratio. Theoretical predictions of the segregating component, based on both bulk phase diagram rule of Burton and Machlin[3] and ε^*-σ^* representation of Abraham and Brundle[1] have also been made for these alloys and the computed data are in good agreement with the experimental results.

4. Surface oxidation

In-situ oxidation of the alloys has been carried out at room temperature and at high temperature so as to form an oxide of at least one element in the alloy. The oxide surface was then heated in vacuum to a higher temperature to check the stability of the oxide formed and to follow the reaction mechanism. The nature of the oxide formed on the surface has been characterised from the metal core level shifts, X-ray-initiated Auger lines such as Cu(L_3VV), Ge(L_3VV), In(MVV), etc., and Cu(L_3VV/$L_3M_{23}M_{23}$) metal Auger intensity ratios.

In the case of the following Cu-based alloys: Cu-Mn, Cu-Ni, Cu-Sn and Cu-In alloys, Cu_2O was formed initially upon oxygen exposure and on further heating in vacuum, displacement reactions such as

$$Cu_2O + Mn \rightarrow 2Cu + MnO$$

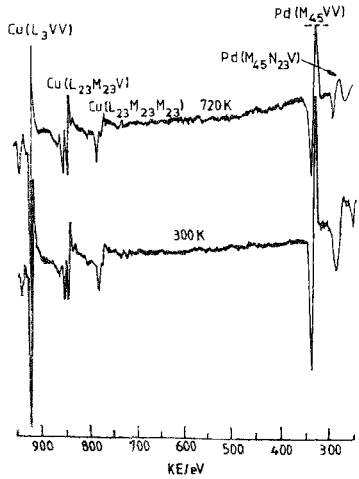

FIG. 1. 3.5 KV electron beam-initiated Auger spectra of Cu-9at.%Pd alloy at 300 and 720 K.

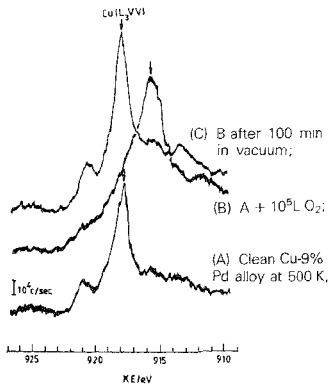

FIG. 2. Al K_α X-ray-initiated Cu (L_3VV) Auger spectra of Cu-9at.%Pd alloy upon oxidation.

occurred on the surface. Cu_2O and GeO were observed on oxidation of Cu-Ge alloy which, on vacuum annealing, led to the reaction

$$Cu_2O + GeO \rightarrow 2Cu + GeO_2.$$

For the first time, GeO phase has been isolated on the surface by following the oxidation of Cu-Ge alloy as well as n-type Ge evaporated films. Cu_2O was seen on Cu-9%Pd alloy at 500 K upon oxygen exposure but on heating at 500 K in vacuum, complete desorption of oxygen was observed, leaving the alloy surface clean (fig. 2). O_2 desorption was confirmed by thermal desorption studies. On Cu-25%Pd and Cu-11%Au alloys only dissociatively chemisorbed oxygen was observed.

Ni-Mn and Ni-Ge alloys showed NiO and oxide of the solute upon oxygen exposure, but on vacuum annealing, the reaction

$$NiO + Mn \rightarrow Ni + MnO$$

occurred on the Ni-Mn alloy surface while Ni-Ge alloy showed desorption of GeO coupled with the reduction of Ni through the reaction

$$NiO + Ge \rightarrow Ni + GeO\ (g)\ \uparrow.$$

On excess oxygen exposure, O^{2-} and O^-(ad) types of oxygen species associated with Ni have been isolated on the Ni-Ru alloy surface. Upon heating conversion of O^{2-} to O^-(ad) leading to O_2 desorption has been observed.

Surface oxidation of ternary alloys has shown a correlation in its behaviour with that of the corresponding binary alloys. The Cu-Ni-Sn alloy, in particular, on oxidation shows Cu_2O, NiO and SnO formation on the surface, but on heating in vacuum, shows stepwise reduction of the oxides as expected.

The formation of the final oxide in all the cases was found to be in accordance with their relative heats of formation. The stability of the chemisorbed structures in addition to thermodynamic considerations seem to play an important role in the formation of the initial oxides.

5. Conclusions

In general, in the case of Cu-based alloys, oxygen can be held as a stable oxide *viz.*, oxide of the solute or can be desorbed depending upon the solute and its segregation behaviour.

References

1. Abraham, F. F. and Brundle, C. R. — Surface segregation in binary solid solutions: A theoretical and experimental perspective, *J. Vacuum Sci. Technol.*, 1981, **18**, 506–519.
2. Forty, A. J. — The structure and chemistry of crystal surfaces, *Contemp. Phys.*, 1983, **24**, 271–299.
3. Burton, J. J. and Machlin, E. S. — Prediction of segregation to alloy surfaces from bulk phase diagrams, *Phys. Rev. Lett.*, 1976, **37**, 1433–1436.

Thesis Abstract (Ph.D.)

Lower-bound limit analysis of footings and slabs on ground by Shashikant Singh.
Research supervisor: K. S. Subba Rao.
Department: Civil Engineering.

1. Introduction

Laterally spread foundations, also known as shallow foundations, are more in practice owing to their economy and simplicity in construction. Whereas considerable progress has been made in the design of superstructures, the design of foundation still needs much attention, understandably due to the added complexity of soil-foundation interaction. The present day knowledge of foundation-soil interaction, contact pressure distribution and collapse loads of foundation structure is still inadequate. Available lower bound solutions are still less in number. The absence is felt more because apart from providing a safe load, lower bound analysis provides the complete distribution of stresses and moments in the structures.

The present thesis is a step towards the limit-state design of shallow foundations and presents many lower-bound limit analysis solutions to the collapse loads of several foundation structures. Only limit state of structural failure has been investigated, as the estimation of collapse load becomes necessary as one of the major inputs for the development of a rational design method. The solutions herein presented are based on the principles of limit analysis using rigid-plastic idealization along with the square yield criterion of failure.

Any analysis of a foundation will require a knowledge of the soil pressure distribution at the interface. Though the non-uniform nature of contact pressure, even for a symmetric system has been demonstrated quite early, the conventional uniform contact pressure is still in current practice because of the difficulties in quantifying the effect of many complex factors that go to define the actual distribution. Nevertheless, attempts made in the past by several investigators give ample evidence to the qualitative nature of the distribution and for most of the foundations met with in practice, the distribution can be generalized by paraboloids. A similar approach has been adopted in the present thesis.

2. Analytical programme

Lower-bound collapse loads have been developed for footings: circular and annular, square and rectangular, continuous and combined, and for large slabs on ground. Some experimental data have been thoroughly analysed to study the development of partial contact in footing. All the three modes of collapse *i.e.*, conical, semi-rigid and rigid have been considered in the analysis in order to understand the behaviour of the footing completely. The existence of shear forces along the boundary resulting from the satisfaction of conditions on moment and the chosen yield criterion have been discussed and duly accounted for. For cases of non-rotational symmetry, a functional approach has been developed. The solution is very efficient for uniform pressure distribution where the whole slab is shown to be yielding. Collapse load of a square footing based on a radial moment field has been successfully developed. Identical upper and lower bound collapse loads have been obtained for continuous and combined footings.

For large slabs, different positions of the load such as at interior, edge or corner, have been considered, and the corresponding collapse loads have been obtained. An expression for the radius of the negative crack has been obtained semi-empirically. For edge and corner cases

approximate solutions, based on a concept of moment reduction, have been developed. Results in terms of their usefulness, limitations, methodology of approach, etc., have been discussed.

3. Results and conclusions

Analysis of experimental data[1] brings out the fact that the separation need not always follow the yield and it can and does start before the yielding of the structure. The closeness of the start of separation and the yield explains the post-yield digging of the slab into the soil in a better manner. In general, separation can take place in three possible ways, *i.e.* preceding the yield, simultaneous with yield and following the yield.

The lifting up of the edges and the associated partial contact will result in a higher collapse load. The increase, however, is not significant for reduction in the contact area from 100% to about 85% of the total area, but the consequent increase in the soil pressure under a circular footing is 1.6 times. The soil pressure shows a five-fold increase when the partial contact factor changes from 1 to 0.6. The safety factor against bearing failure, in such cases, will drastically come down.

A fuller understanding of the behaviour will require examination of all the three possible modes of collapse, namely, conical, semi-rigid and rigid. Earlier researchers[2,3] have considered only conical and rigid modes. Results obtained herein show that the loads corresponding to the conical mode of collapse is the least and as the yield section moves outwards, the loads are higher. The dimension of the loaded area influences the collapse load for conical and semi-rigid modes only and for rigid mode it is the radius of yield hinge that governs the behaviour.

For the case of an edge loaded annular footing, effect of fixity has been incorporated by considering the edges to be fixed with an assignable moment capacity at the edges. This allows the analysis to consider any intermediate degree of fixity. The collapse load variation with the changes in the contact pressure distribution is found to be more significant than that for circular footing. Also for fully fixed edges (equal +ve and −ve moments) the collapse load for annular footings are 48% higher and the spacing between the yield section 60% lesser than for the simply supported case.

For a square footing, the collapse load obtained on the basis of a radial moment field has been found to be very close to the least upper bound and to fall in the region of correct solution identified by Hua Jiang[4]. For rectangular footing a general method has been advanced using the functional approach and a solution has been obtained satisfying the boundary conditions and the yield criterion completely. The solution is very efficient for uniform pressure. For non-uniform pressure, the assumption that M_x and M_y are functions only of X and Y respectively does not lead to efficient solutions.

The soil pressure distribution has a more profound influence on the moment distribution in a continuous footing than on the collapse load. The partial contact, in excess of 85% of the total area, does not seem to affect the load much, but lesser contact areas induce higher stresses in soil. In combined footings, the extent of overhang can be fixed in order to obtain a desired mode of collapse and loads can be calculated. The complete collapse, which depends mainly upon the dimensions of the slab, the spacing of the footing and the relative moment capacities with respect to top and bottom reinforcement, will make the footing the most efficient one.

For interior load on a large slab, the limit analysis solution is developed treating the problem as a rotationally symmetric one and taking the three modes of collapse into consideration. The radius of the negative crack is obtained semi-empirically using the available experimental data as

$b/L = 0.6 + 2.3\ a/L$, in which a is the radius of loaded area and L is the radius of relative stiffness The lower-bound collapse loads thus obtained, show a good closeness to the best upper bounds over the entire range of the loaded region.

For loading other than that in the interior, approximate solutions have been obtained by firs assuming the problem to be of rotational symmetry and then applying a correction to it in the form of a moment reduction factor. The reduction factor is obtained by considering the variation o boundary shear in accordance with the slab boundary and the position of the load. The method results in solutions which compare well with the corresponding upper bounds.

References

1. Shyam Prasad, Y. — *Strength and structural behavior of strip, isolated and combined footings*, Ph.D Thesis, Indian Institute of Science, Bangalore 560 012, India, 1980.
2. Gazetas, G. — Progressive collapse load of rigid-plastic circular foundation, *J. Engng Mech. Div.*, ASCE, 1982, **108**(EM3), 493–508.
3. Meyerhof, G. G. and Subba Rao, K. S. — Collapse load of reinforced concrete footings, *J. Struct. Div.*, ASCE, 1974, **100**(ST5), 1001–1018.
4. Hua Jiang, Da. — Flexural strength of square spread footing, *J. Struct. Div.*, ASCE, 1983, **109**(ST8), 1812–1819.
5. Baumann, R. A. and Weisgerber, F. E. — Yield line analysis of slabs-on-grade, *J. Struct. Div.*, ASCE, 1983, **109**(ST7), 1553–1568.

Thesis Abstract M.Sc. (Engng.)

A compiler writing system based on affix grammars by H. K. Haripriyan.
Research supervisor: Priti Shankar.
Department: Computer Science and Automation.

1. Introduction

Compiler generators have become well established tools in the production of a compiler. In general, a compiler generator takes a specification of a programming language at an abstract level as input and outputs the code for the compiler. While LR, SLR, and LALR grammars are generally used for the specification of the syntax of a programming language, attribute grammars and affix grammars are used commonly to specify the semantics of the language.

The compilers generated by many compiler generators require to scan the input for a parse tree generated from the inputs more than once. Such multipass compilers based on attribute grammars generally require more space and time compared to their one-pass counterparts. Producing one-pass compilers based on LR-parsing of affix grammars was first introduced by Watt[1]. A different approach suggested by Pohlmann[2] has the advantage of both, simplicity, and the ability to parse a larger class of grammars than those covered by Watt's technique.

In this thesis Pohlmann's method has been adapted for implementation. The basic idea is to augment the moves of the LR(k) automation for the grammar, to take into account affix computations. The problem addresed and the algorithms developed are summarized below:

a. Testing an input affix grammar for wellformedness.

b. Implementing a test (the ALR(k) test) to check whether a given affix grammar is deterministically parsable using our technique. The test, originally given by Pohlmann has been implemented with adaptations to make it suitable for application on the LR(k) automation for the grammar. Efficient data structures (for both time and space efficiency) have been designed.

c. Once the input affix grammar has passed the test of (b) it can be used to generate a compiler. A compiler generator has been designed, which has the standard components – namely the driver, and the parsing table. In addition, facilities to generate semantic actions have been incorporated. An existing skeleton facility (consisting of an SLR (1) parser generator) has been enhanced for this purpose. The system designed has been used successfully to generate the front end of a compiler for a PASCAL subset, the grammar for which contains about 60 productions. Based on the experience with the system designed, the merits and disadvantages of the scheme are discussed, space considerations are seen to be critical during the testing phase (*i.e.* during the ALR(k) test).

d. A new algorithm which is an alternative to Pohlmann's ALR(k) test is proposed. this algorithm has a time complexity comparable to that of Pohlmann's, whereas its space requirements are much less.

Reference

1. WATT, D. A., The parsing problem for affix grammars, *Acta informatica*, 1977, **8**, 1–20.

2. POHLMANN, W. LR-parsing for affix grammars, *Acta Informica*, 1983, **20**, 283–300.

Thesis Abstract (M.Sc. Engng)

Micro-computer controlled automatic image focusing system by K. Kalpagam.
Research supervisor: P. S. Naidu.
Department: Electrical Communication Engineering.

1. Introduction

When optical systems are used for producing two-dimensional Fourier transform or images, locating the focused plane is essential, for example, in optical microscopes. Also, many applications like extension of depth of field[1], digital composition of images[2,3], 3-D object shape identification[4], microscopic 3-D imaging[5], etc., involve implementation of algorithms based on some criterion of focus.

2. Theory

Several criteria have been reported in the literature based on the properties of defocused system for use with optical systems illuminated incoherently[4,6,7]. The present work reports a new criterion and a focusing method applicable under coherent, spatially partial coherent and incoherent illuminating conditions. Theoretical analysis shows that entropy is maximum only at

the best focus plane, where ΔI, the difference between maximum and minimum intensities, is maximum. This follows from

$$H_{max} = H - \log\left[\frac{\Delta I}{\Delta I_{max}}\right]$$

where, H represents the information associated with a particular focus state. The expression shows that the observed value of H cannot be greater than the maximum value of H and maximum information is associated with a state having maximum ΔI.

A microcomputer-based automatic focusing system, built around an 8085 microprocessor development board has been used to measure ΔI and locate the plane of best focus.

3. Microcomputer-controlled automatic focusing system

The entire system is built around an 8085 microprocessor. Its functions are:

a) detector positioning
b) image scanning
c) data acquisition in RAM or floppy disc
d) image data analysis
e) lens positioning and
f) interaction with the user through printer and display.

The imaging system is the basic system required for coherent optical processing. By moving the lens, perfect imaging is achieved in the positions

$$V = \frac{1}{2}\left[S \pm \sqrt{S^2 - 4fs}\right] \text{ and } U = (S-V)$$

where, S is the fixed distance between the object and the detector.

The scanning system is centred around a linear photodiode array IPLM512 with 512 diodes with their centres 25.4 μm apart. The array has an integrated self-scanning circuitry and is interfaced to the processor using 12-bit ADC BBADC80 AG12, so that the scanned data is read into the processor memory through program control[8]. The array is mounted upon a leadscrew driven by a stepper controlled by the processor. The position displacement of the array is 2.5 μm for a step angle of 1.8°. The sampling interval in the X and Y directions are determined by the diode aperture size with a minimum of 25.4 μm. The maximum size of the pattern that can be scanned is 10 × 1.3 cm. The lens is also mounted upon a leadscrew, driven by a stepper motor SLOSYN MO61FDO8, interfaced to the processor. The change in the linear position of the lens along the optic axis is 12.5 μm for a step angle of 1.8°.

4. Experimental evaluation of the criterion

A line-drawing and multigrey level object transparencies were used as test objects and the criterion of maximum contrast was studied under coherent and spatially partial coherent illuminating conditions. Results indicated the maximum contrast plane at the geometrical image plane predicted by lenslaw. This is clearly evident from the ΔI *vs* ΔZ plots obtained for $S = 90$ cm (fig. 2). The photographs of the scanned image at various focus states with their corresponding ΔZ values are also shown in fig. 1. Results also proved that the criterion is independent of object and that the maximum contrast parameter obtained by scanning an image segment area of 1×10^{-2} mm^2 covered by as few as 16 diodes of the array is sufficient for

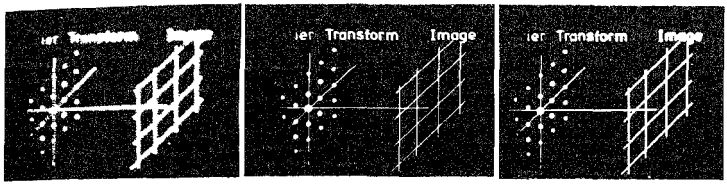

FIG. 1. Focused and defocused pictures of line drawing transparency. Maximum ΔI is associated with the focused image. Arrow indicates the part of the image scanned. a) $\Delta Z = 6.25$ mm, $\Delta I = 2.5$ volts (defocused), b) $\Delta Z = 5$ mm, $\Delta I = 5.45$ volts (focused), c) $\Delta Z = 3.75$ mm, $\Delta I = 4.41$ volts (defocused).

focusing. Under coherent illuminating conditions, the width of the peak at focus, obtained by scanning a line drawing object segment is small compared to that obtained with a multigrey level object segment due to the small depth of focus associated with a line drawing object. Both object segments showed a reduction in the width of the peak under partial coherent illuminating conditions compared to that obtained under coherent case due to decrease in the depth of focus observed in the case of partial coherent illumination. The criterion applied to Fourier transforming operation by a lens also showed the same behaviour near the transform plane. Side lobes were seen on either side of the main peak in all cases with variations occurring in their amplitudes and positions depending on the type of object.

5. Automatic focusing

An algorithm devised for automatic focusing, works in multistages which could be terminated after completion of an integer number of stages depending on the required accuracy and focusing time. Focusing action involves finding the position of the lens for best focus and then moving the lens from its initial position to this detected position. The best focus position is detected from the scanned data by a program by applying the criterion. If Z_i, $i = 1, 2, \ldots p$ are the successive locations of the lens in p-stage focusing operation, the total displacement of the lens with respect to the initial position after p stages is given by,

$$\Delta Z = \sum_{i}^{p} (Z_i - Z_{i-1}).$$

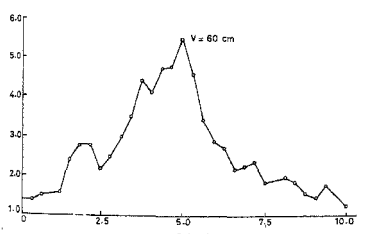

FIG. 2. Plot of ΔI, the difference between maximum and minimum intensities *vs* ΔZ, the defocus parameter, moving the lens in steps of 310 μm, with a line drawing transparency object.

In 3-stage focusing with a final accuracy of 12.5 μm, the time of focusing was approximately 6 sec. at a motor speed of 500 steps/sec. The positional stability was found out by repeating focusing several times, each time measuring the deviation of the lens from its initial position. The standard deviation was found to be 50 μm.

As an application of the method, a Fourier transform lens was positioned to obtain the Fourier transform of a grating (200 lines/mm). Sharp peaks corresponding to grating frequency and its harmonics were obtained for the position of the lens determined by the system using the method explained.

References

1. Pieper, R.J. and Korpel, A. — Image processing for extended depth of field, *Appl. Opt.*, 1983, 22(10), 1449–1453.
2. Sugimoto, S.A. and Ichioka, Y. — Digital composition of images with increased depth of focus considering depth information, *Appl. Opt.*, 1985, **24**(14), 2076–2080.
3. Ghigle, D.C. and Fuckner, M.D. — Technique for conveying three dimensionality from a sequence of image-level slices, *Opt. Soc. Am.*, 1982, 7(3), 116–118.
4. Hausler, G. and Eva Korner — Simple focusing criterion, *Appl. Opt.*, 1984, **23**(15), 2468–2469.
5. Streibl, N. — Depth transfer by an imaging system, *Opt. Acta*, 1984, **31**(11), 1233–1241.
6. Dahne, C. and Lanzl, F. — A microscope focusing technique for a digital image analysing system, *Optik*, 1980, **55**(4), 437–448.
7. Thum, CH. — Measurement of the entropy of an image with application to image focusing, *Opt.Acta*, 1984, **31**(2), 203–211.
8. Reddy, Y. V. Kalpagam, K. and Naidu, P. S. — Microprocessor-controlled photodiode array for measurement of diffraction patterns, *Microprocessors Microsystems*, 1985, **9**(5), 226–230.

Thesis Abstract (M.Sc. Engng)

Track-vehicle interaction of a railway wagon by K. Meera.
Research supervisor: R. Narayana Iyengar.
Department: Civil Engineering.

1. Introduction

Analytical research work undertaken in the field of railway vehicle dynamics entails the development of a suitable system model. The validity of the results drawn from such an analysis depends mainly on how representative the mathematical model is. From a survey of literature, it is found that available track-vehicle interaction studies for Indian railway freight cars do not include the non-linearity of suspension. The present study has been undertaken with this in the background. The freight car considered is the CRT wagon consisting essentially of a wagon body and two wheel-axle sets. Single stage suspension is provided by means of four leaf springs.

A preliminary analysis was first conducted using a linear seven degree-of-freedom model with ıon-proportional damping for the CRT wagon moving over a sinusoidal track. This was with a iew to arrive at first order results which would serve as a reference for the non-linear systems to ıe developed subsequently.

Freight cars in Indian railways have leaf springs which exhibit non-linear hysteretic behaviour. Aore representative models have therefore been developed adapting Bouc's[1] method of ıodelling hysteretic systems. The complexity of the model is increased stagewise.

. Non-linear analysis

or the vehicle modelled as a single degree-of-freedom system with body bounce 'z_b', the on-linear equation of motion is

$$m\ddot{x} + 4K_2x + 4(K_1 - K_2)z = ma\omega^2 \sin\omega t$$
$$\dot{z} + \alpha|\dot{x}|z + \beta|z|\dot{x} = A_2\dot{x}. \tag{1}$$

ere x represents displacement of the wagon body relative to the track undulation, a is the mplitude of track with wavelength λ, K_1 is the small amplitude linear stiffness and K_2 refers to ıe slope at the point where the spring starts hardening, α, β, A_2 are constants which control the ıape of the hysteretic diagram. The non-linear equation of motion has been non-dimensionalised ith respect to δ_e which is the displacement at the point of hardening. The equation is solved ıalytically by the method of slowly varying pafameters.

Equations of motion for a more representative model with four degrees of freedom including ɔunce z_b, pitch ϕ_b of the wagon body, bounce of the leading axle z_1 and bounce of the trailing dle z_t are

$$M_b\ddot{z}_b + 2K_2(z_b + A\phi_b - z_1) + 2K_2(z_b - A\phi_b - z_t) + 2(K_1 - K_2)v_1 + 2(K_1 - K_2)v_t = 0, \tag{2}$$

$$I_b\ddot{\phi}_b + 2AK_2(z_b + A\phi_b - z_1) - 2AK_2(z_b - A\phi_b - z_t) + 2A(K_1 - K_2)v_1 - 2A(K_1 - K_2)v_t = 0, \tag{3}$$

$$M_{AL}\ddot{z}_1 - 2K_2(z_b + A\phi_b - z_1) - 2(K_1 - K_2)v_1 + 2K_tz_1 = 2K_ta \sin\omega t, \tag{4}$$

$$M_{AT}\ddot{z}_t - 2K_2(z_b - A\phi_b - z_t) - 2(K_1 - K_2)v_t + 2K_tz_t = 2K_ta \sin\omega(t - \tau), \tag{5}$$

$$\dot{v}_1 + \alpha|\dot{z}_b + A\dot{\phi}_b - \dot{z}_1|v_1 + \beta|v_1|(\dot{z}_b + A\dot{\phi}_b - \dot{z}_1) = A_2(\dot{z}_b + A\phi_b - \dot{z}_1), \tag{6}$$

$$\dot{v}_t + \alpha|\dot{z}_b - A\dot{\phi}_b - \dot{z}_t|v_t + \beta|v_t|(\dot{z}_b - A\dot{\phi}_b - \dot{z}_t) = A_2(\dot{z}_b - A\dot{\phi}_b - \dot{z}_t). \tag{7}$$

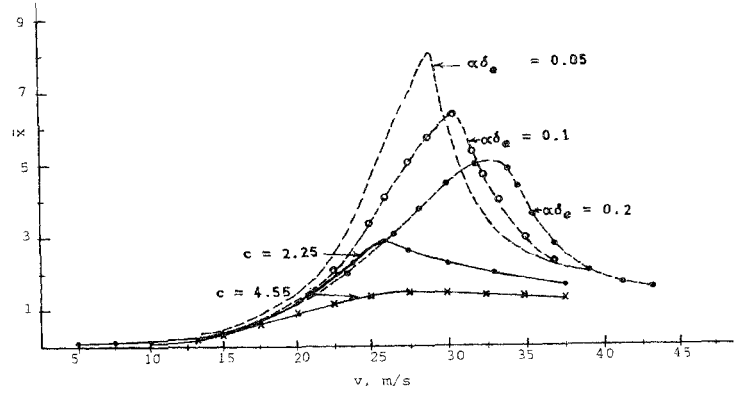

FIG. 1 Variation of bounce amplitude with respect to vehicle velocity.—Linear single degree-of-freedom model; - -Non-linear single degree-of-freedom model $\lambda = 6m$, $a/\delta_e = 1.0$.

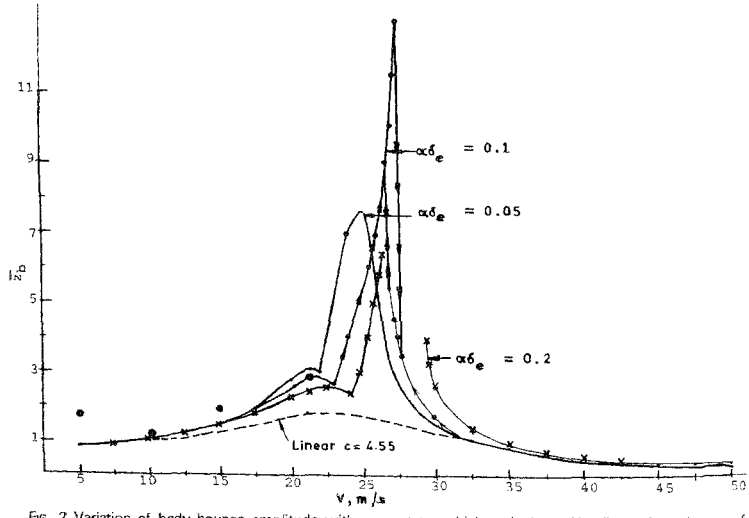

FIG. 2 Variation of body bounce amplitude with respect to vehicle velocity.—Non-linear four degree-of-freedom model; - -Linear four degree-of-freedom model; • • Seven degree-of-freedom non-linear model.

Here v_1, v_t are characteristic non-linear displacements of the leading and trailing springs, M_b, I_p are the mass, pitch inertia of the wagon body, M_{AL}, M_{AT} are the mass of leading and trailing axles and K_t is the track stiffness. These non-linear equations of motion have been non-dimensionalised and solved analytically by equivalent linearisation technique.

While the lateral and vertical motions get uncoupled in a linear model for a vehicle whose centre of gravity coincides with the position of symmetry, the lateral and vertical motions always remain coupled in a non-linear model. Hence more representative seven degree-of-freedom equations of motion have therefore been developed for the freight car which also include the three lateral degrees of freedom namely body roll, leading and trailing axle rolls. Response time histories on these quantities have been obtained by numerical integration.

3. Main results and conclusions

Numerical results have been obtained with reference to certain parametric values which would be consistent with the experimental data available in published literature[2]. Reasonably good fits to the experimental force deflection diagrams are obtained by choosing α, β to be equal and within the range 0.005 to 0.025 and assigning the value 2.0 to (K_2/K_1). For the single degree-of-freedom system, steady-state-frequency-response diagrams have been obtained for variations in these parameters. A comparison between the non-linear and linear response results is shown in fig. 1.

In the four degree-of-freedom model, the effect of varying α, β, on steady-state response has been studied. The system is found to be very sensitive to changes in values of α, β. A comparison of body bounce diagrams for the non-linear and linear four degree-of-freedom models may be seen in fig. 2. Time history information on vehicle response at a few velocities has also been obtained from the accurate seven degree-of-freedom model. These results are compared with other results in fig. 2.

The following conclusions are drawn from the present study:

(i) A linear model for the CRT wagon is inadequate as leaf springs exhibit hysteretic behaviour under dynamic loads.

(ii) Response levels are underestimated in a linear model as can be seen from figs. 1 and 2.

(iii) The non-linear response diagrams for the four degree-of-freedom model show distinct multiple peaks corresponding to the natural frequencies of pitch and bounce. The peaks are shifted to the right indicating a hardening behaviour. Further, the jump phenomenon in the response amplitude is possible for certain combinations of spring parameters and vehicle speed.

References

1. Bouc, R. Forced vibration of a mechanical system with hysteresis, Abstract, *Proc. fourth conf. non-linear oscillation*, Prague, Czechoslovakia, 1967.

2. Desh Deepak *et al* *Evaluation of system parameters, mathematical model of four-wheeled wagon (B. G. CRT) in vertical mode*, R.D.S.O., Report No: MM-7, Progress Report No. 2.